

Poly lactide/graphite nanosheets/MWCNTs nanocomposites with enhanced mechanical, thermal and electrical properties

Jingkuan Duan · Shuangxi Shao · Ya-Li ·
Linfeng Wang · Pingkai Jiang · Baiping Liu

Received: 30 July 2011 / Accepted: 14 November 2011 / Published online: 3 January 2012
© Iran Polymer and Petrochemical Institute 2011

Abstract In this study, we have prepared a series of novel biodegradable polymer [polylactide (PLA)]-based nanocomposites using graphite nanosheets (GNs) and multi-walled carbon nanotubes (MWCNTs) by solution-blending technique and investigated their morphologies, structures, thermal stabilities, mechanical and dielectric properties, and electrical and thermal conductivities. Before preparation of the PLA/GNs/MWCNTs nanocomposites, the raw GNs used were endured a rapid expansion by thermal treatment. Temperature of this treatment had some obvious impacts on morphological changes of graphite nanosheets which were verified by means of scanning electron microscope (SEM) and X-ray diffraction (XRD) techniques. Resultant nanocomposites were characterized and evaluated by means of SEM, XRD, thermal conductivity measurements, tensile and impact tests, thermogravimetric analysis and dielectric measurements. Results obtained in this study indicated that thermal-expanded GNs in the presence of MWCNTs facilitate the formation of an appropriate conductive network in PLA matrix which resulted in a relatively low percolation threshold for thermal and electrical conduction of PLA/GNs/MWCNTs nanocomposites. Significant improvements

in thermal and electrical conductivities, thermal stability and mechanical properties of PLA/GNs/MWCNTs nanocomposites obtained through the presence of both nanoparticles in PLA matrix were associated with their good co-dispersion and co-reinforcement effects. The macroscopic properties of nanocomposites were found to be strongly dependent on their components, concentrations, dispersion, and the resulted morphological structures.

Keywords Polylactide · Graphite nanosheets · MWCNTs · Nanocomposites

Introduction

Poly lactide or poly (lactic acid) (PLA) is a biodegradable aliphatic polyester of lactic acid, a monomeric precursor that can be obtained by natural fermentation from renewable resources, mainly containing starch or sugar. This material has one of the most important situations in the biodegradable polymers market due to its various fields of application. They include a wide variety of biomedical products, packaging materials, fiber production, and more recently, as composites for technical applications. With a tremendous increase in production capacity over the past years, PLA is potentially interesting for engineering applications (electronic and electrical devices, mechanical and automotive parts, etc.) [1–3]. PLA is of increasing interest in industry and academia, because it owns attractive properties comparable with petroleum-based polyolefins [4–6].

Although PLA has balanced properties of mechanical strength, thermal plasticity, and compatibility for short-term commodity applications, the improvement in thermal and mechanical properties of PLA is needed to pursue for

J. Duan (✉) · S. Shao · Ya-Li · L. Wang
Institute of Materials Engineering, Ningbo University
of Technology, Ningbo 315211, People's Republic of China
e-mail: jkduan@sjtu.org

J. Duan · P. Jiang
Shanghai Key Laboratory of Electrical Insulation and Thermal
Aging, Shanghai Jiaotong University,
Shanghai 200240, People's Republic of China

J. Duan · B. Liu
School of Chemical Engineering, East China University
of Science and Technology, Shanghai 200237,
People's Republic of China



long-term high-performance applications. However, the properties of PLA are often not good enough for some applications, such as electronic and electrical devices that require a high level of mechanical properties, thermal and electrical conductivities; thus it requires the tailoring of its properties to reach the end-user demands. Accordingly, many studies on PLA-based nanocomposites have been found that the above drawbacks could be overcome by incorporation of nano-sized particles such as clays and carbon nanotubes [7, 8]. Unfortunately, to the best of our knowledge, studies on PLA-based nanosheets or nanotubes have been carried out limitedly [9] and there are few on preparations of PLA-based nanocomposites using two different nano-fillers, especially, graphite nanosheets and carbon nanotubes (CNTs).

As the molecular-scale tubes of graphitic carbon with outstanding properties, CNTs are among the stiffest and strongest fibers known [10, 11] and hence have attracted much attention for their potential applications in nano-devices, energy conversion, field emission display, nano-electronics, etc. [12, 13]. Of particular interest is recently developed CNTs-based composite nanotechnology consisting of a polymer matrix and well-dispersed CNTs. The obtained polymer/CNTs composites show far improved mechanical properties and conductivity in contrast to those of the pristine polymers, even at very low content of CNTs [14]. But in the literatures, there are few reports regarding the effects of CNTs on electrical and thermal conductivities of bio-composites, simultaneously.

As an alternative to CNTs, graphite nanosheet is also among the leading nano-scale fillers in research and development of commercial products. Graphite nanosheet unites the lower price and layered structure of clays and the superior electrical and thermal properties of CNTs. Thus, it can be an alternative to both clays and CNTs to make polymer composites with competitive multifunctional properties. Graphite nanosheet consisted of graphene nanosheets has thermal and electrical characteristics usually associated with metals which makes it suitable for applications when properties like heat stability, lubricant ability, thermal and electrical conductivities are required [15–17], e.g., electromagnetic interference shields and thermal conductors. However, we have found in literature that graphite nanosheet was associated with CNTs to make conducting polymer composites.

In the recent years, polymer-based nanocomposites reinforced with expanded graphite have shown substantial improvements in mechanical, electrical conductivity and barrier properties in several polymers, such as polyethylene (PE), polyamide 6 (PA6), and polystyrene (PS) [18–20]. The reason is that graphene sheets/layers characterized by high modulus (1TPa) can be separated to a nanometer width, with high aspect ratio (100–1500). Furthermore, the graphite nanosheets can have an enormous surface area (up

to 2,600 m²/g) considering that both sides of the sheets are accessible. Therefore, the dispersion of such nanosheets in a matrix can play a key role in the improvement of both physical and mechanical properties of the resultant nanocomposites [21, 22].

Blending polymer with conducting fillers, such as natural graphite flake, carbon black, and metal powders, to prepare electrically conducting composite has been extensively investigated in the past few decades [23–25]. Conducting polymer composites are great from a practical point of view, because their electrical properties can be tailored by properly choosing components and their relative concentrations. Among the various conducting fillers, naturally abundant graphite, which possesses good electrical conductivity of about 10⁴ S/cm at ambient temperature [26] has been widely used. In most cases, relatively large quantities of graphite are needed to reach the critical percolation value, as the graphite particle size is at micrometer or millimeter scales. Too high concentration of the conductive filler could lead to materials redundancy and detrimental effects on mechanical properties.

To develop a conducting network within PLA matrix with as small amount of filler as possible, we consider using expanded graphite nanosheets and MWCNTs as conducting components to obtain a new bio-based multifunctional “green” product that can be possibly used in different applications related to electric and electronic engineering materials. When different nano-scale conducting fillers are dispersed in PLA matrix, the particular morphology and structure developed provide the advantages of forming the conducting network.

However, relatively little is understood of the compound nano-scale conductive fillers in PLA composites. The aim of the present study was to find out the effects of co-addition of expanded graphite nanosheets and MWCNTs on the macro-properties, e.g., thermal and electrical conductivities and thermal, mechanical and electrical properties, and to establish the correlation between macro-properties and micro-structures of the resultants nanocomposites.

Morphologies, structures, thermal stability, mechanical and electrical properties and thermal conductivity of PLA/GNs/MWCNTs nanocomposites were systematically characterized and measured by adopting scanning electron microscopy, X-ray diffraction method, thermogravimetric analysis, tensile and impact tests, electric resistivity measurements, thermal conductivity measurements, respectively. The experimental results revealed that there were some important effects of co-addition of thermally expanded GNs and MWCNTs on the properties and structures of the resultant nanocomposites. In nanocomposites, a conductive network had formed by the thermally expanded GNs and MWCNTs, and nanocomposites displayed a relatively low percolation threshold for electrical and thermal

conductivities. Due to the existence of the conducting network, mechanical, thermal stabilities, thermal and electrical conductivities of PLA had been improved obviously.

Experimental

Materials

A commercially available poly (lactic acid) (PLA, 4032D) was supplied from Nature Works LLC (UAS) with a number average molecular weight [M_n (PLA)] of 58,000 g/mol, D-isomer content about 1.5% and polydispersity index (PI) of 2.1. The graphite nanosheets (GNs) used in this research were offered from Xiamen Knano Graphite Co. Ltd. (China). GNs with an aspect ratio of about 100 (average diameter of 5 μm and average thickness of 50 nm) were prepared by an ultra-sonication powdering technique [21]. MWCNTs (MFG Code M2) were purchased from Chengdu Organic Chemicals Co. Ltd., Chinese Academy of Sciences (China) with outside diameter (OD) of 8–15 nm and length of about 50 μm , special surface area (SSA) $>233 \text{ m}^2/\text{g}$ and electrical conductivity (EC) $>10^2 \text{ s/cm}$.

The thermal expansion process of graphite nanosheets

The expanded graphite nanosheet was obtained by a rapid thermal expansion of GNs. Prior to the mixing step, GNs were put into an oven that was maintained at the different temperatures and taken out after 3 min to produce the expanded graphite nanosheet. Upon rapid heating, the GNs were expanded explosively several hundred times along the thickness direction due to the evaporation of the intercalant and the thermal shock. The expanded GNs were immersed in high-purity chloroform and ultrasonicated at 70 w and 42 kHz for 8 h to obtain the exfoliated graphite nanosheets.

Preparation of PLA/GNs/MWCNTs nanocomposites

Hybrid composite specimens were prepared by the process suggested in the literature [27] which involved the use of a solvent. PLA/GNs/MWCNTs composites were prepared according to the following steps. According to the formulation in Table 1, the preweighed graphite nanosheet, MWCNTs and high-purity chloroform were loaded into a big tube. The tube with a high stir was placed into an ultrasonic bath with water as the coupling fluid. Ultrasonic irradiation and thoroughly stirring (about 5,000 turns/min) were then applied and maintained for 3 h to obtain a suspension of the expanded GNs filled by MWCNTs. Then, the solution of PLA in high-purity chloroform was added into the mixture. The suspension consisting PLA and expanded GNs filled by MWCNTs was roughly stirred and ultra-sonicated for at least

Table 1 Formulation of PLA/GNs/MWCNTs nanocomposite

Samples	PLA (pbw) ^a	MWCNTs (pbw)	GNs (pbw)
PLA	100	–	–
PLA/C 0.5/G 0.5	100	0.25	0.25
PLA/C1/G1	100	0.5	0.5
PLA/C 1.5/G1.5	100	1.5	1.5

^a Part by weight

3 h at ambient temperature to obtain the homogeneous dispersion of expanded GNs filled by MWCNTs within PLA. Finally, the uniform mixture was subjected to degassing at 120 °C for 5 h to remove the solvent. Subsequently, the polymer material containing the fillers was then molded. The nanocomposites with various amounts of graphite nanosheets and MWCNTs were prepared via this procedure.

Characterizations and measurements

Scanning electron microscopy

The morphological features of the pristine GNs, MWCNTs, MWCNTs filled GNs, and PLA/GNs/MWCNTs nanocomposites were characterized using a scanning electron microscope (JSM-7401F, JEOL Ltd., Japan). The powders of the pristine GNs, MWCNTs, and the expanded GNs were dissolved into high-purity chloroform, and underwent ultrasonication for 2 h, following: the resulting suspensions were poured onto conductive metal columns. At last, these columns were subjected to degassing at 120 °C for 2 h to remove the solvent, and then were observed by SEM. The PLA/GNs/MWCNTs nanocomposites were prepared for SEM by fracturing the melt-quenched composite films in a liquid nitrogen bath, then, fractured sample surfaces were coated with gold–palladium sheet.

Wide X-ray diffraction

Information on nano-scale structures of the pristine GNs, the GNs filled by MWCNTs, and PLA/GNs/MWCNTs nanocomposites was obtained by X-ray diffraction using $\text{CuK}\alpha$ radiation ($\lambda = 1.5418 \text{ \AA}$) (D/max-2200/PC). The diffraction patterns were collected from 10° to 50° (2θ) at a scanning rate of 3°/min.

Thermogravimetry analysis

Thermal stability of PLA/GNs/MWCNTs nanocomposites was carried out on 10 mg samples by a thermogravimetric analyzer (TGA Q500, TA Instrument, USA) at heating rate of 10 °C/min from room temperature to 600 °C under air



flow ($60 \text{ cm}^3/\text{min}$). The thermal degradation temperatures taken into account were the onset degradation temperature, the temperature at 50% of weight loss ($T_{0.5}$) and the temperature of maximum weight loss rate (PDT).

Thermal conductivity

Thermal conductivities of PLA/GNs/MWCNTs nanocomposites were measured on the LFA447 (Netzsch, Germany) nanoflash diffusivity instrument. The sample dimensions were approximately $10 \times 10 \times 1 \text{ cm}$. Measurement of the thermal diffusivity, specific heat and density allows the calculation of the thermal conductivity.

Electrical resistivity

The volume electrical resistivity of PLA/GNs/MWCNTs nanocomposites was measured with an electrometer/high-resistance meter (ZC36, Shanghai Cany Precision Instrument Co. Ltd., China) at room temperature. The electrical contacts to the electrodes were ensured with gold layer deposits onto both (top and bottom) surfaces of the dumbbell shaped samples by a sputtering technique. The measurements were repeated eight times to obtain the averaged electrical resistivity of any sample.

Mechanical properties

Mechanical properties of PLA/GNs/MWCNTs nanocomposites such as tensile strength and elongation-at-break were performed using a universal testing machine (Xin Sansi Co. Ltd., China) at room temperature according to GB/T1040-2009 at a speed rate of 50 mm/min . All tests were carried out by at least ten samples previously conditioned for 48 h at $23 \pm 2 \text{ }^\circ\text{C}$ and a relative humidity of $50 \pm 2\%$.

Notched impact strength measurements of PLA/GNs/MWCNTs nanocomposites were performed by an Izod Ray-Ran 2500 pendulum impact tester (4 J, UK) and a notching instrument in accordance to the ASTM D256 (Method A, impact rate = 3.46 m/s and 0.668 kg hammer). All tests were carried out by at least ten samples previously conditioned in similar conditions for tensile measurements.

Result and discussion

Thermal expansion of graphite nanosheets

The exfoliation phenomena of the graphite intercalated compounds (GICs) have been investigated for long time. There are several methods to expand GICs. It has been

reported that thermal expansion process is one of the most effective methods to exfoliate graphite nanoplatelets into graphene [28–31]. To investigate the detailed morphological changes of graphite nanosheets due to thermal expansion, SEM micrographs of the pristine graphite nanosheets (GNs) and GNs treated at different temperatures were obtained and are presented in Figs. 1 and 2, respectively. SEM micrograph of the MWCNTs used is shown in Fig. 3, as well.

It was confirmed that the pristine GNs were constituted of flakes which was approximately platelet of average diameter of $5 \text{ }\mu\text{m}$ and average thickness of 50 nm , with an aspect ratio of about 100 (Fig. 1a, b). On the other hand, compared with the GNs treated by thermal expansion (Fig. 2), the pristine GNs were detected to have greater diameter and rougher surface topology owing to the acid treatment.

After GNs endured a thermal treatment process, the final product of GNs was characterized to have the diameter of about $4 \text{ }\mu\text{m}$ and a smooth surface which could be attributed to the evaporation of materials from the surface of the

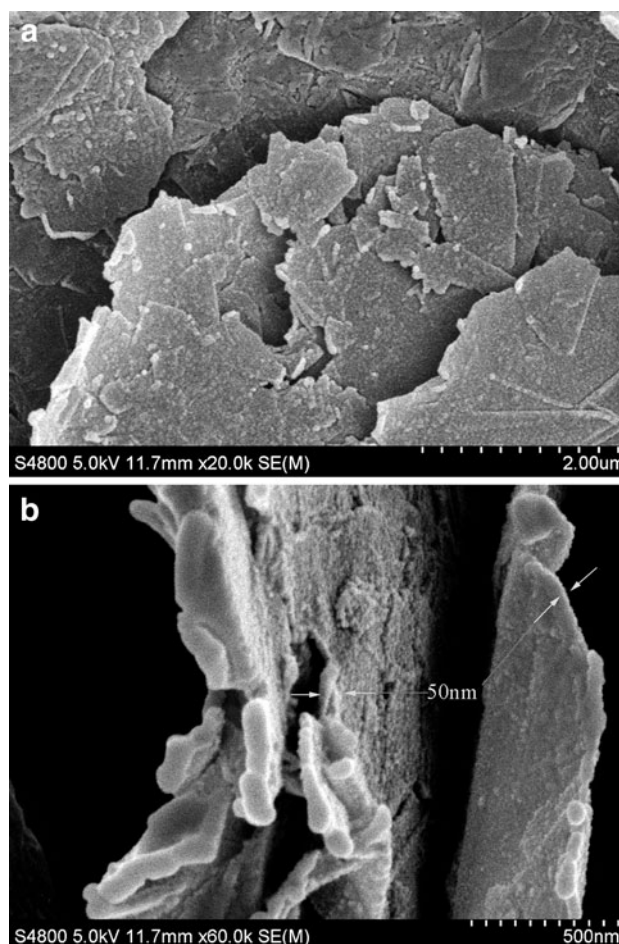


Fig. 1 SEM micrographs of the pristine graphite nanosheets: direction perpendicular (a) and direction parallel (b)

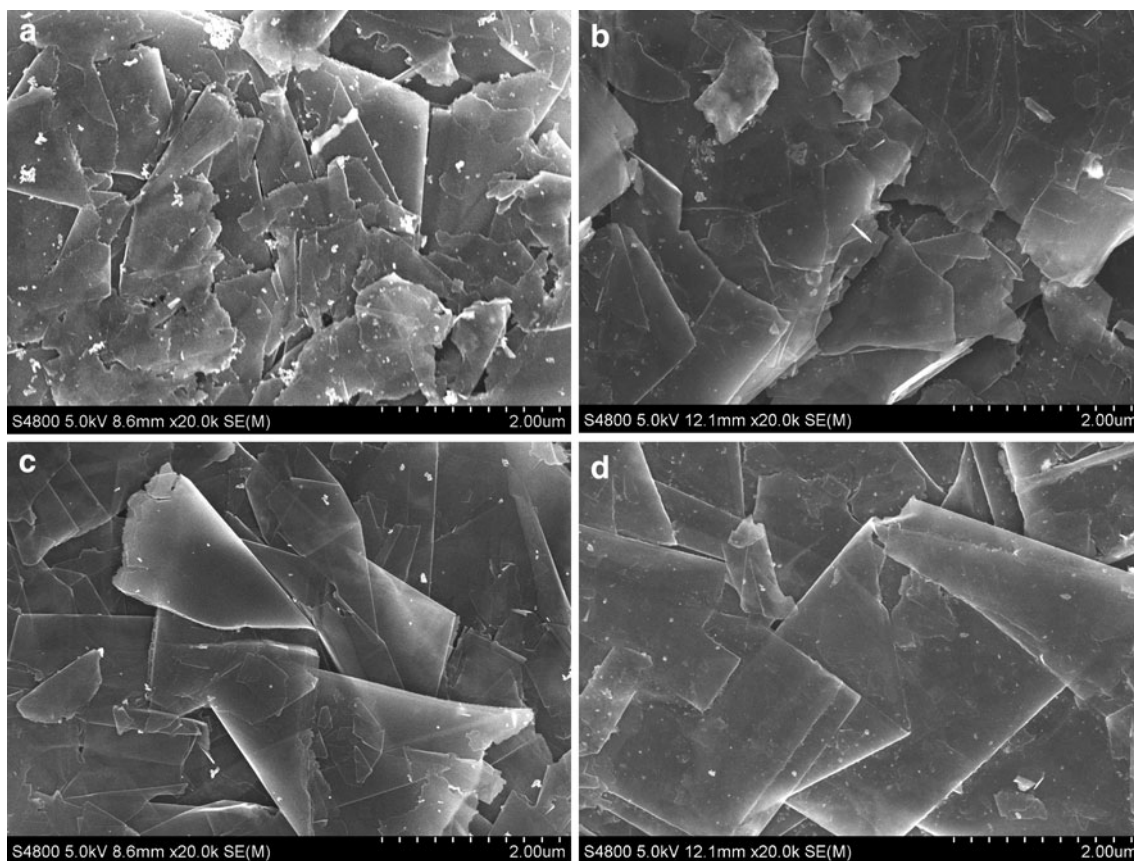


Fig. 2 SEM micrographs of the treated graphite nanosheets at: 300 °C (a), 500 °C (b), 700 °C (c), and 800 °C (d)

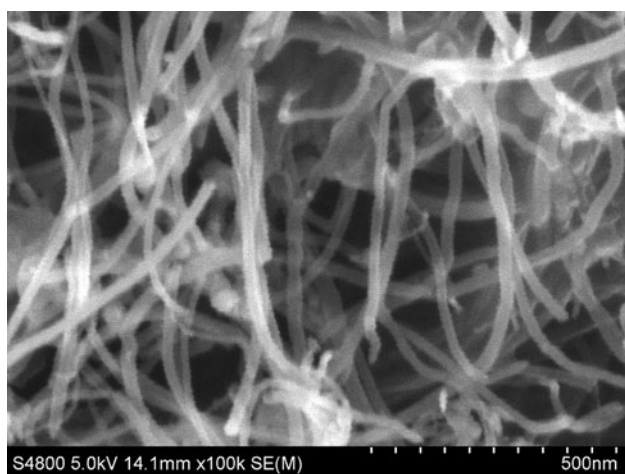


Fig. 3 SEM micrograph of MWCNTs

pristine GNs. In addition, it was clearly found that the nanosheets had been partially exfoliated, and the higher the treating temperature, the exfoliated extent was more as can be seen in Fig. 2.

To examine the structural features and exfoliated extents of the GNs treated by different temperatures, their X-ray diffraction patterns were obtained, as shown in Fig. 4. GNs

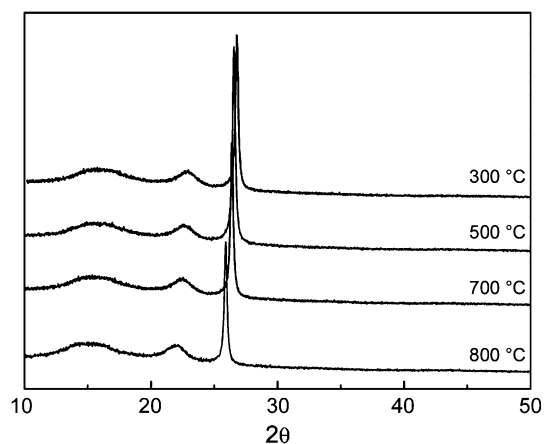


Fig. 4 X-ray diffraction patterns of GNs treated at different temperatures

exhibited an obviously sharp diffraction peak at $2\theta = 27.1^\circ - 25.5^\circ$, which is corresponding to the d_{002} . With increase of the treating temperatures from 300 to 800 °C, the d-spacing of thermally treated GNs gradually increased from 3.38 to 3.58 nm. This result is in accordance with the findings in Fig. 3. This phenomenon could be due to the rapid evaporation of CO_2 and H_2O from the surfaces of the



pristine GNs, and the higher treating temperatures led to the larger distances between nanosheets.

Microstructure of graphite nanosheets filled by MWCNTs

To further understand and investigate the effects of both thermal treatment process and addition of MWCNTs into GNs on the expanded extent of the pristine GNs, the certain amount (~ 0.05 g) of the pristine GNs, MWCNTs, GNs treated by thermal expansion, and the mixture of 0.05 g MWCNTs and 0.05 g GNs treated by thermal expansion were solved into high-purity chloroform, and after these suspensions were slightly stirred, these mixtures were limpidlyquescently placed for 5 h.

The resultant suspensions are shown in Fig. 5. It is clear from Fig. 5 that the volume of GNs which had undergone thermal-expanded process was obviously larger than that of the pristine GNs. It is surprised to find out that addition of MWCNTs into the GNs treated by thermal expansion resulted to the volume expansion of GNs, further. And after ultra-sonication, the volume of the mixture of MWCNTs and GNs treated by thermal expanded process grow further. Some conclusions could be easily drawn from these phenomena: (1) thermal expanded process is one of effective methods to exfoliate graphite nanoplatelets; (2) addition of MWCNTs into GNs could contribute to exfoliation or expansion of GNs; (3) the microwave process could give a better degree of expansion of GNs and MWCNTs.

From above results, it was very reasonable to think that ultra-sonication process could promote incorporation of MWCNTs into the graphite nanosheets that underwent thermal expansion in solvent. This prediction had been verified by SEM micrographs as shown in Fig. 6, which displays the mixture of MWCNTs and GNs treated by thermal process at 500 °C (ratio of MWCNTs and GNs is 1). From Fig. 6, it is obviously found out that MWCNTs were homogeneously dispersed among the graphite



Fig. 5 States of MWCNTs, pristine GNs, GNs treated by thermal expansion, and mixtures of GN sand MWCNTs with and without ultra-sonication, in high-purity chloroform

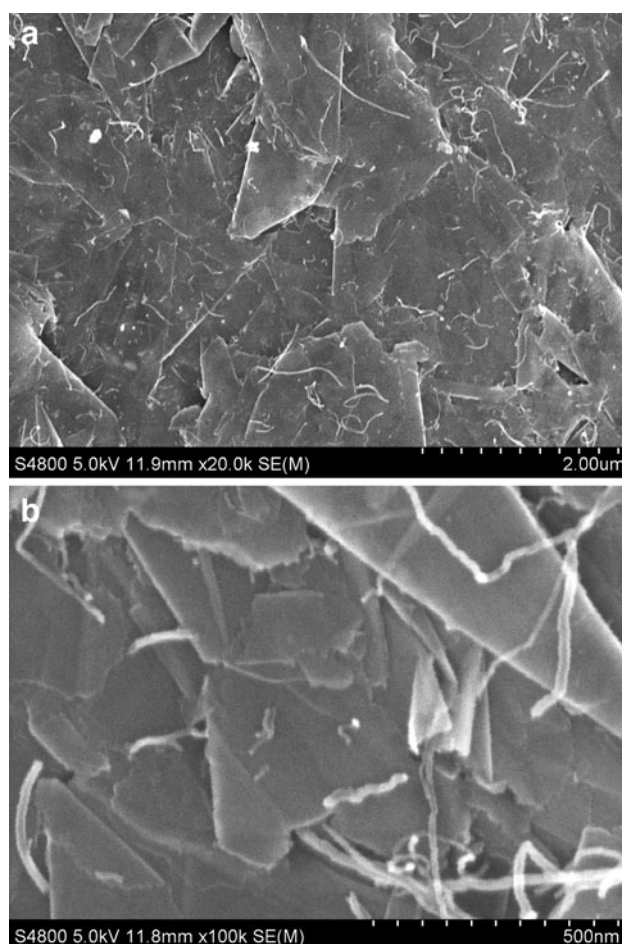


Fig. 6 SEM micrographs of the dispersion states of the mixture of MWCNTs and GNs treated by thermal process at 500 °C (MWCNTs/GN = 1) at **a** $\times 20,000$ and **b** $\times 100,000$ magnifications

nanosheets, and a carbon network had been formed by GNs and MWCNTs.

Microstructures of PLA/GN/MWCNTs nanocomposites

To maintain the resultant networks structure of GNs/MWCNTs and to make applicable devices, filling PLA in the networks-shape was very important. Figure. 7a, b shows the SEM micrographs of the fractured surfaces of PLA/GNs/MWCNTs nanocomposites which contain 0.5 pbw graphite and 0.5 pbw MWCNTs.

It can be seen that PLA/GNs/MWCNTs nanocomposites with 0.5 pbw of GNs and 0.5pbw of MWCNTs exhibited a relative rough fractured surface without any aggregates of GNs and MWCNTs particles as shown in Fig. 7. It confirmed that graphene nanoplatelets of GNs and MWCNTs were dispersed almost homogeneously in PLA matrix (Fig. 7a) and the MWCNTs were displaced between GNs platelets as shown in Fig. 7b. From these results, it is easy

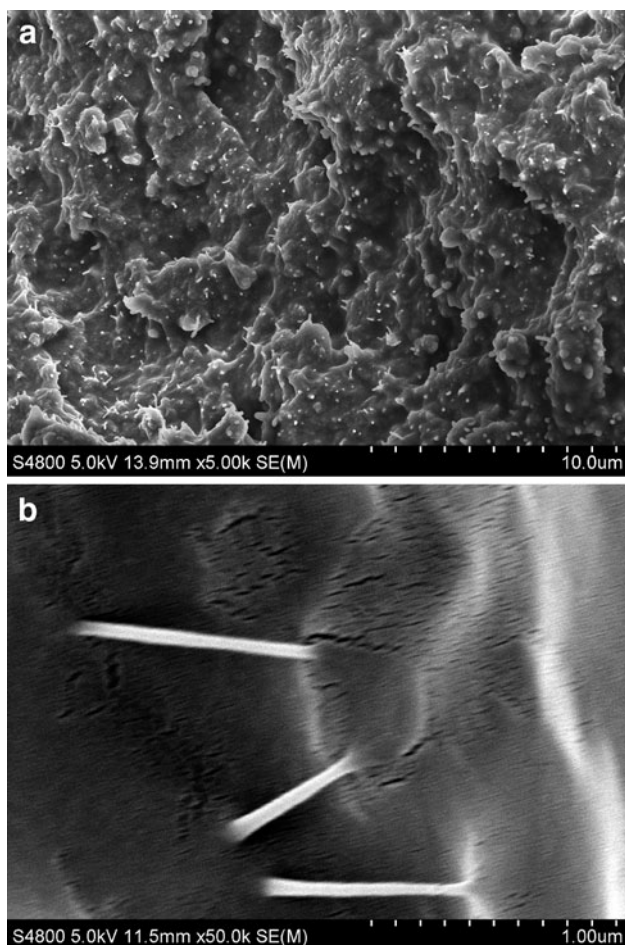


Fig. 7 SEM micrographs of the fracture surfaces of PLA/GNs/MWCNTs nanocomposites at 0.5 pbw of GN and 0.5 pbw of MWCNTs at: **a** $\times 5,000$ and **b** $\times 50,000$ magnifications

to draw a conclusion that the network consisting graphite nanosheets and MWCNTs had been formed in composites.

During the preparation of nanocomposites, blade of the homogenizer rotated and broke the large graphite flakes

into even smaller ones. The application of ultra-sonication further improved the dispersion of graphite nanosheets and MWCNTs in PLA matrix. The rough stirring and ultra-sonication might have resulted in the permeation of MWCNTs into the expanded graphite nanosheets.

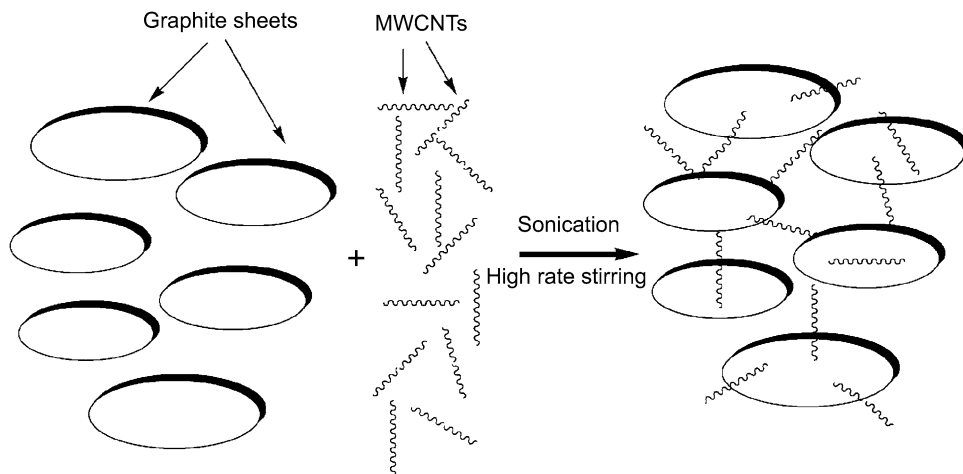
As a summary, a roadmap describing the microstructure formation of the PLA/EG/MWCNTs nanocomposites during the processing is presented in Scheme 1. When GNs were heated, expansion took place in the locations where oxidation occurred, resulting in a porous structure in the graphite flakes (Fig. 2), therefore, the expanded graphite was formed. The MWCNTs had been impregnated into graphite sheets during ultra-sonication and stirring, which led to the formation of conductivity network based on MWCNTs and graphite sheets. Due to Van der Waals force between GNs and MWCNTs, a stabilized C-network was formed at last. When the MWCNTs-filled GNs was mixed with PLA matrix thoroughly by stirring and sonication, the PLA/EG/MWCNTs nanocomposite with interpenetrated GNs/MWCNTs network had been obtained, finally.

WXR D

To examine the structure features of GNs, X-ray diffraction patterns of the pristine GNs, the GNs underwent thermal expansion, and the GNs filled by MWCNTs with and without ultrasonication treatment were obtained, as shown in Fig. 9.

Since graphite materials have a layered structure, they show characteristic peaks in their WXR D patterns, among these, the peak from d002 is the highest and the most distinctive one, appearing at $2\theta \approx 26.5^\circ$. It is well known that the height of the d002 is a measure of how many layers are stacking together to form graphite flakes. Thus, the degree of exfoliation is investigated by measuring the d002 peak height after the exfoliation process. The greater the number of unintercalated layers, the more intense the X-ray

Scheme 1 The model of the carbon network based on GNs and MWCNTs



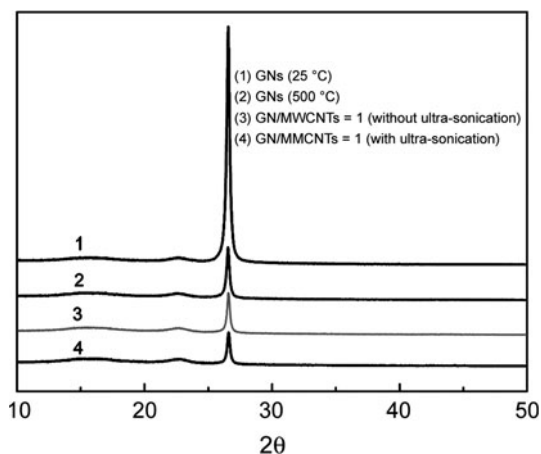


Fig. 8 X-ray diffraction patterns of: 1 the graphite nanosheets (GNs), 2 GNs treated by heat, 3 GNs filled by MWCNTs without ultra-sonication, 4 GNs filled by MWCNTs with ultra-sonication

diffraction peak for crystalline graphite [32]. From Fig. 8, it is clear that the pristine GNs (25 °C) exhibits a sharp and strong diffraction peak at $2\theta = 26.5^\circ$.

After the GNs underwent the thermally expansion treatment at 500 °C for 3 min, the diffraction peak of the GNs is a very weaker peak. After the GNs, which had endured the thermal expansion at 500 °C for 3 min, were filled by MWCNTs (GNs/MWCNTs = 1) without ultra-sonication, its diffraction peak is almost equal to that of the GNs treated by thermal expansion treatment at 500 °C for 3 min. However, after the GNs filled by MWCNTs underwent an ultrasonication, the GNs displayed the weakest peak among all the GNs samples. It was worth pointing out that similar results had been previously reported and the peak observed at 26.5° with reduced intensity was associated to lower number of remaining aggregates and to a reduced number of graphite layers in the former case [33]. These phenomena indicated that the GNs could be partially exfoliated into graphite nanoplatelets by means of both thermal expansion process and incorporation of MWCNTs into the GNs, and these results were in agreement with the SEM micrographs as shown in Figs. 5 and 6.

To investigate the structural feature of PLA/GNs/MWCNTs nanocomposites, X-ray diffraction patterns of different nanocomposites were obtained, as presented in Fig. 9. It is clearly seen that PLA/GNs/MWCNTs nanocomposites exhibited an initial broad diffraction peak at $2\theta = 16.5^\circ$ which may be corresponded to PLA crystalline structure [34] and another clear sharp diffraction peak at $2\theta = 26.5^\circ$ owing to the GNs particles is detected for PLA/GNs/MWCNTs nanocomposites, even at very low GNs and MWCNTs concentration of 0.25 pbw, respectively. It means that the GNs particles remained in a poor crystalline state in nanocomposites, being intercalated or exfoliated during the

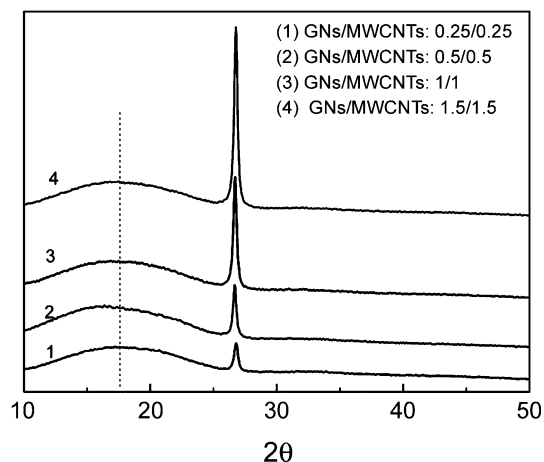


Fig. 9 X-ray diffraction patterns of PLA/GNs/MWCNTs nanocomposites at various MWCNTs concentrations

solvent-mixing process [35]. The presence of the sharp peak at 26.5° confirms not only the presence of the pure graphite based stacks of parallel graphene sheets but also the fact that the solvent-compounding applied here was able to exfoliate or completely separate the grapheme layers. Although some sheets still exist in aggregate forms. Accordingly, the increased intensity recorded at higher conductive fillers contents could be attributed to the higher number of graphene layers organized in stacks. In addition, these results also revealed that the concentration of expanded graphite nanosheets filled by MWCNTs makes an important impact on the number of the long-range order of graphite nanosheets.

It is valid to say that graphite nanoplatelets were successfully prepared by both the thermal expansion treatment and the incorporation of MWCNTs into GNs, thus could be used as the multifunctional reinforcing nanoparticles for PLA-based nanocomposites.

Mechanical properties of PLA/GNs/MWCNTs nanocomposites

Tensile mechanical properties of PLA/GNs/MWCNTs nanocomposites containing various graphite nanosheets and MWCNTs contents were examined at room temperature, as shown in Fig. 10, which presents tensile strength and elongation-at-break values of nanocomposites as a function of graphite nanosheets and MWCNTs content. From Fig. 10, it is found that the elongation-at-break values of the nanocomposites gradually decrease with increase of conductive fillers concentration as compared to that of pure PLA. Values of the elongation-at-break decrease from 20% for pure PLA sample to 15% for the nanocomposite sample with 1.5 pbw of GNs and MWCNTs. It seems that the high decreases in the elongation-at-break values of PLA/GNs/MWCNTs nanocomposites are proved owing to



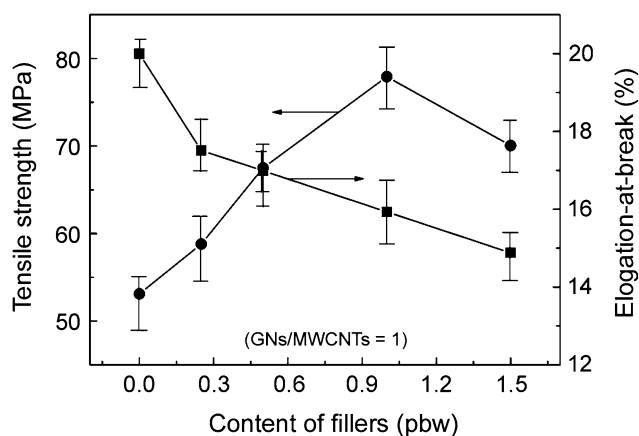


Fig. 10 Mechanical properties of PLA/GNs/MWCNTs nanocomposites at various conductive fillers concentrations

the hardening effect of graphite nanoplatelets in the PLA matrix [35].

The tensile strength of PLA was measured be ~ 54 MPa, as can be seen in Fig. 10. For PLA/GNs/MWCNTs nanocomposites, the tensile strength increased initially to ~ 78 MPa at 1 pbw GNs and 1 pbw MWCNTs, remains constant up to 1.5 pbw GNs and 1 pbw MWCNTs, but decreases slightly at higher fillers contents. Nonetheless, the tensile strength of PLA/GNs/MWCNTs nanocomposites is still higher than that of the PLA matrix. Figure 11 shows stress–strain curves of PLA/GNs/MWCNTs nanocomposites at various conductive fillers. From Fig. 11, it is found that for PLA/GNs/MWCNTs nanocomposites, the strain-at-break decreases with increasing the fillers contents (GNs/MWCNTs = 1). It seems that the high decreases in strain-at-break values of PLA/GNs/MWCNTs nanocomposites are proved owing to the hardening effect of fillers in the PLA matrix.

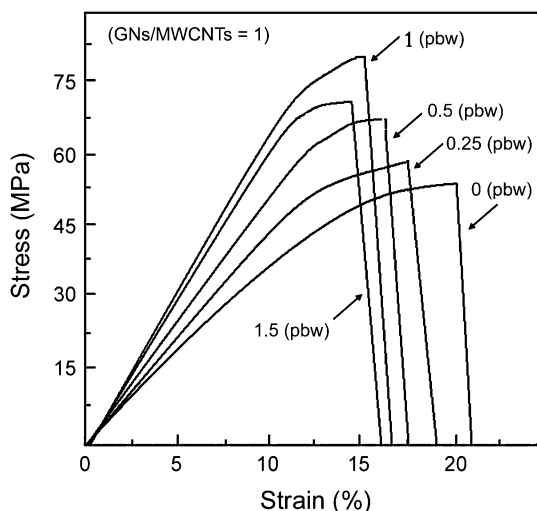


Fig. 11 Stress–strain curves of PLA/GNs/MWCNTs nanocomposites for various conductive fillers concentrations

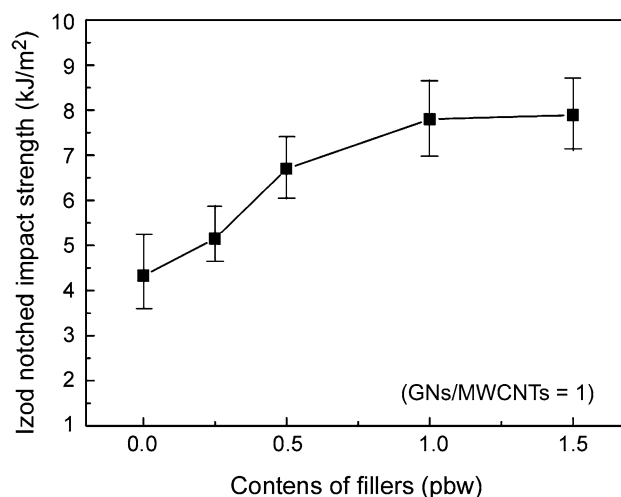


Fig. 12 Impact properties of PLA/GNs/MWCNTs nanocomposites

Impact properties are key factors that basically decide the suitability of a material for usage in structural application. Figure 12 shows the impact fracture strengths of the different PLA/GNs/MWCNTs nanocomposites. It can be seen from Fig. 12 that the impact strength values of the all PLA/GNs/MWCNTs nanocomposites are higher than that of the pure PLA, but the impact strength values increase gradually with the increase of conductive fillers in the PLA matrix. The noticeable improvement of impact properties for PLA/GNs/MWCNTs nanocomposites could be owing to the reinforcing effects of graphite nanoplatelets incorporated with MWCNTs which dispersed homogeneously in the PLA matrix.

Additionally, we pointed out that the nanoscopic gaps had a direct correspondence to the morphology and structure of the filler–filler bonds. Because of confinement effects, the polymer chains in nanoscopic gaps between two attractive filler surfaces were strongly immobilized implying that the filler–filler bonds are consisted of glassy-like, immobilized polymer bridges between adjacent filler particles. In particular, it implies that the filler–filler bonds were quite stiff to allow the transmittance of stress along the fillers network. The gap distance corresponds to the length of filler–filler bonds which in turn impacts on the stiffness and strength of the bonds and hence the whole fillers network. These explanations may be used to interpret the mechanical properties of the PLA/GNs/MWCNTs nanocomposites.

Thermal stability of PLA/GNs/MWCNTs nanocomposites

TGA was conducted to investigate the effect of the conductive fillers (GNs filled by MWCNTs) on the thermal stability behavior of the PLA/GNs/MWCNTs nanocomposite samples

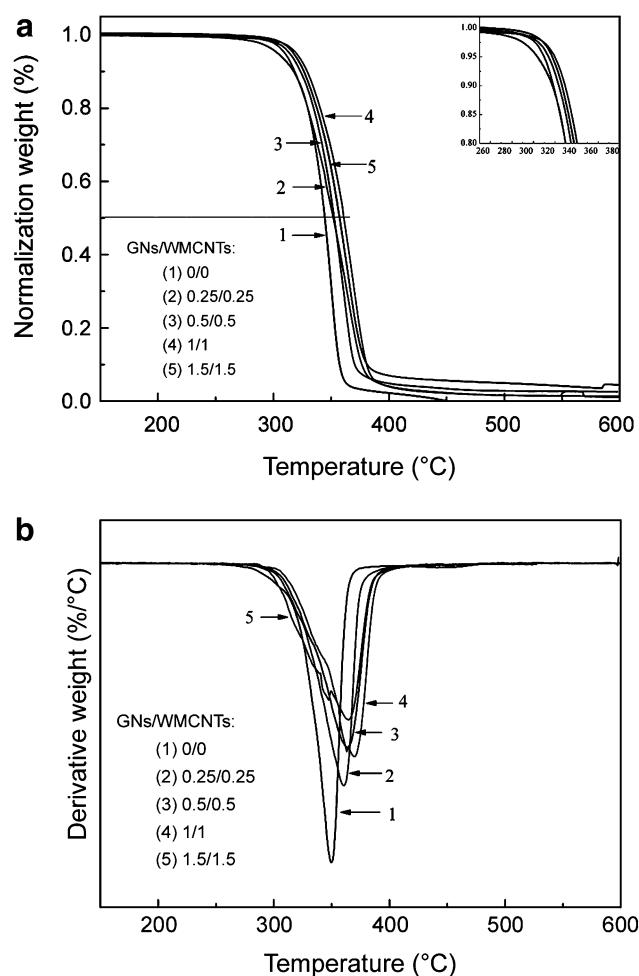


Fig. 13 Thermal stability curves of pure PLA and PLA/GNs/MWCNTs nanocomposite at different loadings of conductive fillers: TGA (a); DTG (b)

and the pristine PLA. Figure 13a, b shows TGA and corresponding differential Thermogravimetric (DTG) thermograms of pure PLA and PLA/GNs/MWCNTs nanocomposites at different conductive fillers loading, respectively.

For quantitative comparison of the thermal stabilities among different PLA/GNs/MWCNTs nanocomposites, the onset decomposed temperature (T_{set}), the thermal degradation temperatures of 50% weight losses ($T_{0.5}$), the maximum temperature of degradation [PDT(max)] and Char yield (%) up to 500 °C were evaluated from TGA and DTG thermograms which are summarized in Table 2.

As shown in Fig. 13a and Table 2, it can be seen that compared to that of the pure PLA, the TGA curves of the nanocomposites are shifted toward higher temperatures. The onset temperature of thermal degradation of the nanocomposite sample with conductive fillers loading 0.5 pbw is significantly increased from 279.8 to 286.9 °C. Addition of GNs filled by MWCNTs into PLA led to the distinctly gradual improvement in decomposition onset

Table 2 Thermal properties of different nanocomposites (under air flow and heating rate of 10 °C/min)

Samples	T_{set} (°C)	$T_{0.5}$ (°C)	PDT (max) (°C)	Char yielded up to 500 °C (%)
PLA	279.8	344.16	349.9	0
PLA/C 0.5/G0.5	288.3	351.7	368.8	2.5
PLA/C1/G1	299.2	360.9	369.7	2.7
PLA/C 1.5/G1.5	299.9	358.6	366.9	4.4

temperature for PLA/GNs/MWCNTs nanocomposites with the increase of conductive filler concentration.

The peak decomposition temperature of the DTG curve represented the temperature at which the maximum weight loss rate is reached, as shown in Fig. 13b. The peak decomposition temperature of the nanocomposite appears above 360.3 °C and is increased about 10 °C compared to that of the pure PLA. The thermal degradation temperatures of 50% weight losses ($T_{0.5}$) also display a marked enhancement in different nanocomposite samples compared to that of the neat PLA. It should be pointed out that a dramatic increase of thermal stability is observed for nanocomposites with increasing the fillers contents. Such effect in thermal stability has been previously reported in case of graphite dispersion in other polymer matrices [36–38].

The improved thermal stability of PLA/GNs/MWCNTs nanocomposites is believed to originate from the following facts: (1) essential increase of thermal resistance is mainly connected to the retardation effect of the conductive network based on the expanded GNs and MWCNTs, on the motion of molecules of PLA during heating-up; (2) shielding effect conferred by the flake-like nanofiller, in fact, the layers of GNs are thought to increase the diffusion pathways of the degradation by-products and the good thermal stability could be associated to hindered diffusion of volatile decomposition products; (3) presence of the dispersed GNs filled by MWCNTs in PLA matrix possibly accelerates the PLA crystallization, significantly.

Conductivity of PLA/GNs/MWCNTs nanocomposites

As mentioned at the very beginning of this study, the ultimate goal of making a renewable, sustainable, biodegradable, and eco-friendly composite was to develop lightweight highly conductive materials. To determine the conductive performances of the PLA/EG/MWCNTs nanocomposites prepared in the present study, both the volume electrical resistivities and thermal conductivity of testing sheets made from PLA/EG/MWCNTs nanocomposites were measured at room temperature. The results are presented in Figs. 14 and 15, respectively.

It is obvious from the Figs. 14 and 15 that the addition of GNs filled by MWCNTs has a significant effect on the

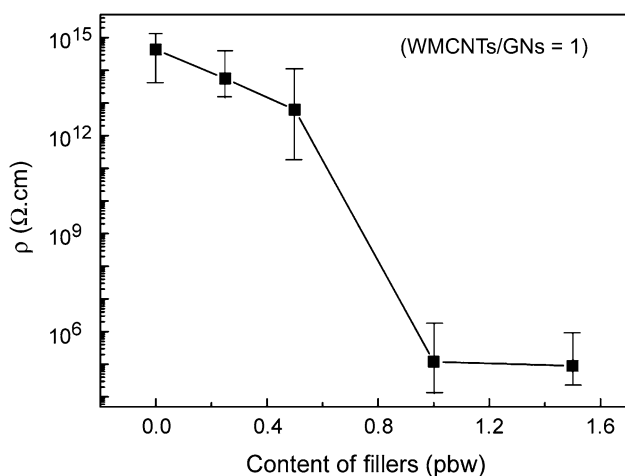


Fig. 14 Volume electrical resistivity of PLA/GNs/MWCNTs nanocomposites at different loadings of conductive fillers

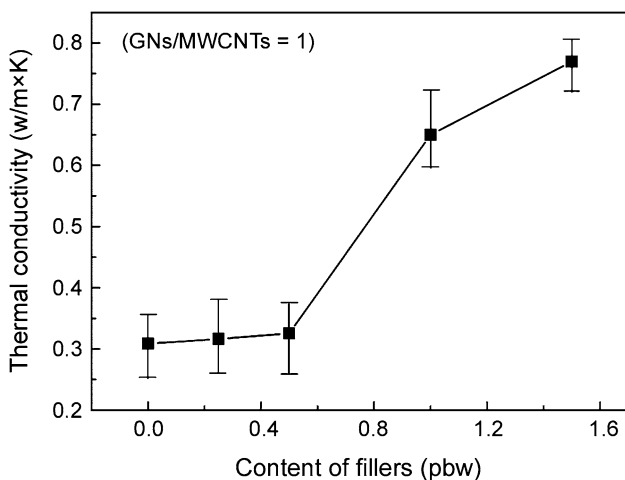


Fig. 15 Heat conductivity of PLA/GNs/MWCNTs nanocomposites at different loadings of conductive fillers

thermal and electrical conductions of PLA matrix. Upon the conductive fillers loading, the thermal and the volume electrical resistivities were dramatically increased as compared to that of pure PLA matrix.

Figure 14 shows clearly that with increase of the GNs/MWCNTs contents, the volume electrical resistivities of PLA/GNs/MWCNTs nanocomposites gradually reduces, and when the ratio of GNs/MWCNTs goes beyond 0.5/0.5, the volume electrical resistivity of PLA/GNs/MWCNTs nanocomposite reduces dramatically. For comparison, when 1 pbw of fillers (MWCNTs/GNs = 1) was incorporated into PLA, the volume resistivity of the nanocomposite would be about 10 orders of magnitude lower than that of the pure PLA, then with the increase in the amount of fillers, the volume resistivity of

nanocomposites decreased slowly. This phenomenon demonstrated that the percolation threshold for conductivity of the nanocomposites is lower than 1 pbw. The microstructures as shown in the above figures revealed that low value of percolation threshold might be mainly attributed to better conductive network consisting of GNs and MWCNTs with special morphology. There exists contact resistance in the percolating network formed within nanocomposites, as well.

Additionally, it is important to notice that the volume electrical resistivity of $\sim 10^5 \Omega \text{cm}^{-1}$ for PLA/GNs/MWCNTs nanocomposite is low enough to attain the electrostatic dissipation and/or partial electromagnetic dissipation for thermoplastics, fibers, and films.

Figure 15 shows the variation in thermal conductivity of the nanocomposites with respect to the fillers contents. It can be seen that thermal conductivity increases at higher GNs concentration. It indicates that the mean carbon free path and conductive network produced by adding of the GNs filled by MWCNTs, strongly improved the transport routes necessary for high-thermal conductance.

Conclusion

To allow PLA utilization in technical applications, addition of selected nano-fillers into this biodegradable polyester represented a good alternative for enhancing its performances. In this study, graphite nanosheets were pretreated by rapid thermal expansion and then solvent compounded with MWCNTs, including a PLA solution under ultra-sonication to prepare a novel kind of PLA-based nanocomposites. The results indicated that for graphite nanosheets, both the thermal expansion process and addition of MWCNTs were the most useful methods to obtain a highly efficient, stabilized and practical conductive network in polymer matrix. It was confirmed by X-ray diffraction patterns and SEM micrographs that the disordered GNs and MWCNTs in PLA/GNs/MWCNTs nanocomposites were homogeneously dispersed in the PLA matrix without forming any aggregates. However, micro-sized GN particles in PLA/GNs/MWCNTs nanocomposites maintained their original crystalline state; it led to the relative low electrical and thermal percolation threshold of PLA/GNs/MWCNTs nanocomposites. Compared to pure PLA, the resultant PLA/GNs/MWCNTs nanocomposites displayed significant improvements in the thermal stability and mechanical properties.

Acknowledgment The authors gratefully acknowledge the financial support of China Postdoctoral Science Foundation under the grant no. 20100470755, and also thank partly the financial supports of Scientific and Technical Innovation Plan of Undergraduate of Zhejiang Province (2010) (No: NG 18) for this research.



References

- Lindblad MS, Liu Y, Albertsson AC, Ranucci E, Karlsson S (2002) Polymers from Renewable Resources. *Adv Polym Sci* 157:139–161
- Wang Y, Qi R, Xiong C, Huang M (2011) Effects of coupling agent and interfacial modifiers on mechanical properties of poly(lactic acid) and wood flour biocomposites. *Iran Polym J* 20:281–294
- Lemmouchi Y, Murariu M, Dos Santos AM, Amass AJ, Schacht E, Dubois P (2009) Plasticization of poly(lactide) with blends of tributyl citrate and low molecular weight poly(D, L-lactide)-b-poly(ethylene glycol) copolymers. *Eur Polym J* 45:2839–2848
- Drumright RE, Gruber PR, Henton DE (2000) Poly(lactic acid) technology. *Adv Mater* 12:1841–1846
- Martin O, Avérous L (2001) Poly(lactic acid): Plasticization and properties of biodegradable multiphase systems. *Polymer* 42:6209–6219
- Tsuji H (2002) Poly(lactides). In: Doi Y, Steinbuchel A (eds) *Polyesters III: Applications and Commercial Products*, Vol 4. Wiley, Weinheim, 129–177
- Yoon JT, Jeong YG, Lee SC, Min BG (2009) Influences of poly(lactic acid)-grafted carbon nanotube on thermal, mechanical, and electrical properties of poly(lactic acid). *Polym Adv Technol* 20:631–638
- Villmow T, Pötschke P, Pegel S, Häußler L, Kretzschmar B (2008) Influence of twin-screw extrusion conditions on the dispersion of multi-walled carbon nanotubes in a poly(lactic acid) matrix. *Polymer* 49:3500–3509
- Miloaga DG, Hosein H-AA, Rich MJ, Kjoller K, Drzal LT (2008) Scanning probe thermal analysis of poly(lactic acid)/exfoliated graphite nanoplatelet (xGnPTM) nanocomposites. *J Biobased Mater Bio* 2:78–84
- Iijima S (1991) Helical microtubules of graphitic carbon. *Nature* 354:56–58
- Salvetat JP, Briggs GAD, Bonard J-M, Bacsá RR, Kulik AJ, Stöckli T, Burnham NA, Forró L (1999) Elastic and shear moduli of single-walled carbon nanotube ropes. *Phys Rev Lett* 82:944–947
- Subramoney S (1998) Novel nanocarbons: structure, properties, and potential applications. *Adv Mater* 10:1157–1173
- Yousefi AA (2011) Hybrid poly(vinylidene fluoride)/nanoclay/MWCNT nanocomposites: PVDF crystalline transformation. *Iran Polym J* 20:725–733
- Andrews R, Weisenberger MC (2004) Carbon nanotube polymer composites. *Curr Opin Solid State Mater Sci* 8:31–37
- Zhao YF, Xiao M, Wang SJ, Ge XC, Meng YZ (2007) Preparation and properties of electrically conductive PPS/expanded graphite nanocomposites. *Compos Sci Technol* 67:2528–2534
- Ciallella C, Gruenberger TM, Grivei E, Probst N (2008) Expanded graphite offers new opportunities. *Plast Additiv Compound* 10:40–41
- Kalaitzidou K, Fukushima H, Drzal LT (2007) A new compounding method for exfoliated graphite-polypropylene nanocomposites with enhanced flexural properties and lower percolation threshold. *Compos Sci Technol* 67:2045–2051
- Li J, Kim J-K, Sham ML (2005) Conductive graphite nanoplatelet/epoxy nanocomposites: effect of exfoliation and UV/ozone treatment of graphite. *Scripta Mater* 53:235–240
- Zheng W, Wong S-C, Sue H-J (2002) Transport behavior of PMMA/expanded graphite nanocomposites. *Polymer* 43:6767–6773
- Huang JH, Baired DG, McGrath JE (2005) Development of fuel cell bipolar plates from graphite filled wet-lay thermoplastic composite materials. *J Power Sources* 150:110–119
- Chen GH, Weng WG, Wu DJ, Wu CL, Lu JR, Wang PP, Chen XF (2004) Preparation and characterization of graphite nanosheets from ultrasonic powdering technique. *Carbon* 42:753–759
- Chen GH, Wu DJ, Weng WG, Wu CL (2003) Exfoliation of graphite flake and its nanocomposites. *Carbon* 41:619–621
- Li J, Vaisman LD, Marom G, Kim JK (2007) Br treated graphite nanoplatelets for improved electrical conductivity of polymer composites. *Carbon* 45:744–750
- Panwar V, Mehra RM (2008) Study of electrical and dielectric properties of styrene-acrylonitrile/graphite sheets composites. *Eur Polym J* 44:2367–2375
- Lu JG, Moon K-S, Xu JW, Wong CP (2006) Synthesis and dielectric properties of novel high-K polymer composites containing in situ formed silver nanoparticles for embedded capacitor applications. *J Mater Chem* 16:1543–1548
- King JA, Tucker KW, Vogt BD, Weber EH, Quan CL (1999) Electrically and thermally conductive nylon 6, 6. *Polym Compos* 20:643–654
- Lu X, Xu G (1997) Thermally conductive polymer composites for electronic packaging. *J Appl Polym Sci* 65:2733–2738
- Chung DDL (1987) Review: exfoliation of graphite. *J Mater Sci* 22:4190–4198
- Jang BZ, Zhamu A (2008) Processing of nanographene platelets (NGPs) and NGP nanocomposites: a review. *J Mater Sci* 43:5092–5101
- George JJ, Bhadra S, Bhowmick AK (2010) Influence of carbon-based nanofillers on the electrical and dielectric properties of ethylene vinyl acetate nanocomposites. *Polym Compos* 31:218–225
- Steurer P, Wissert R, Thomann R, Mülhaupt R (2009) Functionalized graphenes and thermoplastic nanocomposites based upon expanded graphite oxide. *Macromol Rapid Commun* 30:316–327
- Kim H, Hahn HT, Viculis LM, Gilje S, Kaner RB (2007) Electrical conductivity of graphite/polystyrene composites made from potassium intercalated graphite. *Carbon* 45:1578–1582
- Yasmin A, Luo J-J, Daniel IM (2006) Processing of expanded graphite reinforced polymer nanocomposites. *Compos Sci Technol* 66:1179–1186
- Pluta M (2004) Morphology and properties of polylactide modified by thermal treatment, filling with layered silicates and plasticization. *Polymer* 45:8239–8251
- Kim I-H, Jeong YG (2010) Poly(lactide)/exfoliated graphite nanocomposites with enhanced thermal stability, mechanical modulus, and electrical conductivity. *J Polym Sci Polym Phys* 48:850–858
- Zhao YF, Xiao M, Wang SJ, Ge XC, Meng YZ (2007) Preparation and properties of electrically conductive PPS/expanded graphite nanocomposites. *Compos Sci Technol* 67:2528–2534
- Lim L-T, Auras R, Rubino M (2008) Processing technologies for poly(lactic acid). *Prog Polym Sci* 33:820–852
- Uhl FM, Yao Q, Nakajima H, Manias E, Wilkie CA (2005) Expandable graphite/polyamide-6 nanocomposites. *Polym Degrad Stab* 89:70–84